*In blessed memory of Professor A.P. Favorskii*

# Numerical Simulation of Three-Dimensional Quasi-Neutral Gas Flows Based on Smoothed Magnetohydrodynamic Equations

## T. G. Elizarova[a] and M. V. Popov[a, b]

[a] *Keldysh Institute of Applied Mathematics, Russian Academy of Sciences, Miusskaya pl. 4, Moscow, 125047 Russia*
[b] *École Normale Supérieure de Lyon, CRAL (UMR CNRS 5574), Université de Lyon 1,*
*46 allee d'Italie 69007 Lyon, France*
*e-mail: telizar@mail.ru, mikhail.v.popov@gmail.com*
Received January 26, 2015

**Abstract**—A new finite-difference method for the numerical simulation of compressible MHD flows is presented, which is applicable to a broad class of problems. The method relies on the magnetic quasi-gasdynamic equations (referred to as quasi-MHD (QMHD) equations), which are, in fact, the system of Navier–Stokes equations and Faraday's laws averaged over a short time interval. The QMHD equations are discretized on a grid with the help of central differences. The averaging procedure makes it possible to stabilize the numerical solution and to avoid additional limiting procedures (flux limiters, etc.). The magnetic field is ensured to be free of divergence by applying Stokes' theorem. Numerical results are presented for 3D test problems: a central blast in a magnetic field, the interaction of a shock wave with a cloud, and the three-dimensional Orszag–Tang vortex. Additionally, preliminary numerical results for a magnetic pinch in plasma are demonstrated.

## 1. INTRODUCTION

In this paper we present a numerical algorithm and simulation results obtained for unsteady three-dimensional flows of an ideal quasi-neutral plasma in the field of electromagnetic forces. The algorithm is an extension of previously constructed finite-difference schemes based on the quasi-gasdynamic (QGD) equations for viscous compressible gas flows [1−3]. This work is closely related to the research interests of Professor Favorskii, who, as a renowned expert in the computational fluid dynamics, actively supported a then nascent scientific area whose development has led to the formation of the QGD approach. As the head of a scientific school in computational MHD, Professor Favorskii would have appreciated the results presented below.

The QGD equations express the conservation laws for gasdynamic variables, namely, the density, momentum components, and energy averaged over a short time interval. It is assumed that an averaged quantity is a smooth function of time, which can be expanded in a Taylor series about every time $t$, i.e.,

$$\overline{f}(r,t) = \frac{1}{\tau} \int_{t}^{t+\tau} f(r,t')dt' \approx f(r,t) + \tau\frac{\partial f(r,t)}{\partial t} + \dots . \tag{1}$$

The conservation law for the averaged quantity $\overline{f}(r,t)$ must contain terms reflecting the conservation of $f(r,t)$ and of a correction term proportional to a small parameter $\tau$ that has the dimension of time. Thus, the QGD equations represent the Navier–Stokes equations involving additional dissipative terms. These terms play a stabilizing role in the numerical solution of the equations, since they introduce additional dissipation.

The QGD equations with allowance for magnetic fields were first considered in [3, 4] for the description of viscous gas and fluid flows. The effect of a magnetic field was taken into account in the form of magnetic forces and dissipative $\tau$-correction terms in the gas dynamics part, while the field itself was described by Maxwell's equations without $\tau$-correction. For this system, an entropy balance equation was

constructed, the exact solution of the Hartman problem was obtained, and the flow of an electrically conducting melt was computed in the no induction approximation.

The above described averaging procedure can also be applied to the magnetic field equations written in the framework of the unified MHD system. Due to this approach, magnetic viscous flows would be described with the help of quasi-gasdynamic equations for magnetohydrodynamics (referred to as quasi-MHD (QMHD) equations) in a self-consistent form. Such equations were first considered in [5, 6], where they were examined as applied to standard 1D and 2D tests, namely, the Riemann problem, propagation of magnetic waves, the dissipation and decay of a Alfven wave, a blast wave in a magnetized medium, the Orszag–Tang vortex, and the interaction of a shock wave with a cloud. In all the cases, the numerical solution was demonstrated to converge well to the exact solution in the case of mesh refinement.

In [7] the QMHD equations were extended to the case of the nonideal gas equation of state in the presence of external forces and a heat source. A heat balance equation was derived, and the entropy properties of the QMHD equations were examined.

In this paper, we present the system of QMHD equations in the 3D case written componentwise and describe numerical results for 3D test problems, such as a central blast in a magnetic field, the interaction of a shock wave with a cloud, and the three-dimensional Orszag–Tang vortex. Additionally, preliminary numerical results are demonstrated for a plasma pinch confined by a longitudinal magnetic field. The stability of a pinch is a major problem in plasma confinement within magnetic traps.

## 2. QMHD EQUATIONS

The QMHD equations are written in a Cartesian coordinate system with use of the following standard notation for independent variables: $\rho$ is the density; $u_x$, $u_y$, and $u_z$ are the velocity components; $B_x$, $B_y$, and $B_z$ are the magnetic flux density components; and $E$ is the total energy per unit volume.

For the squared magnitudes of the velocity and magnetic flux density, we use the brief notation

$$u^2 = u_x^2 + u_y^2 + u_z^2, \quad B^2 = B_x^2 + B_y^2 + B_z^2.$$

The factor $\sqrt{1/4\pi}$ was included in the definition of the magnetic field $\mathbf{B}$. In this notation, the total energy per unit volume is written as

$$E = \rho\varepsilon + \frac{\rho u^2}{2} + \frac{B^2}{2},$$

where $\varepsilon$ is the specific internal energy. To make the system of equations closed, we need an equation of state. For the case of an ideal gas, it has the form $p = (\gamma - 1)\rho\varepsilon$, where $p$ is the gasdynamic pressure and $\gamma$ is the ratio of specific heats. The equation of state expressed in terms of temperature has the form $p = \rho RT/\eta$, where $R$ is the universal gas constant and $\eta$ is the mean molecular weight of the gas. From this, the temperature $T$ is expressed as $T = p\eta/\rho R$.

A combination of $E$, $p$, and $\rho$ gives the total specific enthalpy:

$$H = (E + p)/\rho.$$

The small parameter with respect to which we perform averaging is denoted by $\tau$; it has the dimension of time (see (1)). For convenience, the second term in the Taylor expansion in (1) is denoted as the increment $\Delta$:

$$\overline{f} = f + \Delta f.$$

Let us write out the increments of all the quantities to be used in what follows. These expressions are derived from the MHD equations for an inviscid non-heat-conducting quasi-neutral plasma [8]:

$$\Delta\frac{1}{\rho} = -\tau\left(\mathbf{u}\mathrm{grad}\frac{1}{\rho} - \frac{1}{\rho}\mathrm{div}\mathbf{u}\right),$$

$$\Delta\varepsilon = -\tau\left(\mathbf{u}\mathrm{grad}\varepsilon + \frac{p}{\rho}\mathrm{div}\mathbf{u}\right), \quad \Delta p = -\tau\left(\mathbf{u}\mathrm{grad}p + \gamma p\mathrm{div}\mathbf{u}\right),$$

$$\Delta u_i = -\tau\left[\mathbf{u}\mathrm{grad}u_i + \frac{1}{\rho}\frac{\partial}{\partial i}\left(p + \frac{B^2}{2}\right) - \frac{1}{\rho}\left(\frac{\partial B_x B_i}{\partial x} + \frac{\partial B_y B_i}{\partial y} + \frac{\partial B_z B_i}{\partial z}\right)\right],$$

$$\Delta B_i = \tau \left[ \frac{\partial}{\partial x}(B_x u_i - u_x B_i) + \frac{\partial}{\partial y}(B_y u_i - u_y B_i) + \frac{\partial}{\partial z}(B_z u_i - u_z B_i) \right],$$

where $i = x, y, z$ and $\mathbf{u}$ is the velocity vector. The scalar product of the velocity with the gradient of $f$ and the divergence of the velocity are given by

$$\mathbf{u}\,\mathrm{grad}\,f = u_x \frac{\partial f}{\partial x} + u_y \frac{\partial f}{\partial y} + u_z \frac{\partial f}{\partial z},$$

$$\mathrm{div}\,\mathbf{u} = \frac{\partial u_x}{\partial x} + \frac{\partial u_y}{\partial y} + \frac{\partial u_z}{\partial z}.$$

The mass conservation law in the framework of the QMHD system is written as

$$\frac{\partial \rho}{\partial t} + \frac{\partial j_x}{\partial x} + \frac{\partial j_y}{\partial y} + \frac{\partial j_z}{\partial z} = 0, \tag{2}$$

where the fluxes are corrected components of the mass flux density:

$$j_i = \rho(u_i - w_i), \quad i = x, y, z.$$

The correction value is proportional to $\tau$ and is written in terns of spatial derivatives, which are, in fact, the derivatives of fluxes in the Euler equation for MHD:

$$w_x = \frac{\tau}{\rho} \left\{ \frac{\partial}{\partial x}\left( \rho u_x^2 + p + \frac{B^2}{2} - B_x^2 \right) + \frac{\partial}{\partial y}(\rho u_y u_x - B_y B_x) + \frac{\partial}{\partial z}(\rho u_z u_x - B_z B_x) \right\},$$

$$w_y = \frac{\tau}{\rho} \left\{ \frac{\partial}{\partial x}(\rho u_x u_y - B_x B_y) + \frac{\partial}{\partial y}\left( \rho u_y^2 + p + \frac{B^2}{2} - B_y^2 \right) + \frac{\partial}{\partial z}(\rho u_z u_y - B_z B_y) \right\},$$

$$w_z = \frac{\tau}{\rho} \left\{ \frac{\partial}{\partial x}(\rho u_x u_z - B_x B_z) + \frac{\partial}{\partial y}(\rho u_y u_z - B_y B_z) + \frac{\partial}{\partial z}\left( \rho u_z^2 + p + \frac{B^2}{2} - B_z^2 \right) \right\}.$$

The conservation laws for the momentum components have the form

$$\frac{\partial \rho u_i}{\partial t} + \frac{\partial T_{xi}}{\partial x} + \frac{\partial T_{yi}}{\partial y} + \frac{\partial T_{zi}}{\partial z} = \frac{\partial \Pi_{xi}}{\partial x} + \frac{\partial \Pi_{yi}}{\partial y} + \frac{\partial \Pi_{zi}}{\partial z}, \tag{3}$$

where $i = x, y, z$. The components of the tensor $T_{ij}$ ($i, j = x, y, z$) express the force associated with the corrected momentum flux and the gasdynamic and magnetic pressure in each direction:

$$T_{ij} = \begin{pmatrix} j_x u_x + p + \frac{1}{2}B^2 - B_x^2 & j_y u_x - B_y B_x & j_z u_x - B_z B_x \\[2mm] j_x u_y - B_x B_y & j_y u_y + p + \frac{1}{2}B^2 - B_y^2 & j_z u_y - B_z B_y \\[2mm] j_x u_z - B_x B_z & j_y u_z - B_y B_z & j_z u_z + p + \frac{1}{2}B^2 - B_z^2 \end{pmatrix}.$$

Here and below, the first and second indices are the column and row numbers, respectively. The tensor $\Pi_{ij}$ ($i, j = x, y, z$) includes the Navier–Stokes viscous stress tensor $\Pi_{ij}^{ns}$, which is proportional to the dynamic viscosity $\mu$, and the tensor $\Pi_{ij}^{qmhd}$ associated with QMHD correction terms proportional to $\tau$:

$$\Pi_{ij} = \Pi_{ij}^{ns} + \Pi_{ij}^{qmhd}, \tag{4}$$

where

$$\Pi_{ij}^{ns} = \begin{pmatrix} \dfrac{4}{3}\dfrac{\partial u_x}{\partial x} - \dfrac{2}{3}\dfrac{\partial u_y}{\partial y} - \dfrac{2}{3}\dfrac{\partial u_z}{\partial z} & \dfrac{\partial u_y}{\partial x} + \dfrac{\partial u_x}{\partial y} & \dfrac{\partial u_z}{\partial x} + \dfrac{\partial u_x}{\partial z} \\[2mm] \dfrac{\partial u_y}{\partial x} + \dfrac{\partial u_x}{\partial y} & \dfrac{4}{3}\dfrac{\partial u_y}{\partial y} - \dfrac{2}{3}\dfrac{\partial u_x}{\partial x} - \dfrac{2}{3}\dfrac{\partial u_z}{\partial z} & \dfrac{\partial u_y}{\partial z} + \dfrac{\partial u_z}{\partial y} \\[2mm] \dfrac{\partial u_z}{\partial x} + \dfrac{\partial u_x}{\partial z} & \dfrac{\partial u_y}{\partial z} + \dfrac{\partial u_z}{\partial y} & \dfrac{4}{3}\dfrac{\partial u_z}{\partial z} - \dfrac{2}{3}\dfrac{\partial u_x}{\partial x} - \dfrac{2}{3}\dfrac{\partial u_y}{\partial y} \end{pmatrix}.$$

Note that $\Pi_{ij}^{ns} = \Pi_{ji}^{ns}$ and the diagonal terms are

$$\Pi_{ii}^{ns} = \mu\left(2\frac{\partial u_i}{\partial i} - \frac{2}{3}\mathrm{div}\mathbf{u}\right), \quad i = x, y, z.$$

Tensor $\Pi_{ij}^{qmhd}$ in (4) is written as

$$\Pi_{ij}^{qmhd} = \begin{pmatrix} -\rho u_x\Delta u_x - \Delta p - \dfrac{\Delta(B^2)}{2} + \Delta(B_x^2) & -\rho u_y\Delta u_x + \Delta(B_y B_x) & -\rho u_z\Delta u_x + \Delta(B_z B_x) \\[2mm] -\rho u_x\Delta u_y + \Delta(B_x B_y) & -\rho u_y\Delta u_y - \Delta p - \dfrac{\Delta(B^2)}{2} + \Delta(B_y^2) & -\rho u_z\Delta u_y + \Delta(B_z B_y) \\[2mm] -\rho u_x\Delta u_z + \Delta(B_x B_z) & -\rho u_y\Delta u_z + \Delta(B_y B_z) & -\rho u_z\Delta u_z - \Delta p - \dfrac{\Delta(B^2)}{2} + \Delta(B_z^2) \end{pmatrix}.$$

To the increment $\Delta$, we apply differentiation rules according to which $\Delta ab = a\Delta b + b\Delta a$.

The magnetic filed equations have the form

$$\frac{\partial B_i}{\partial t} + \frac{\partial T_{xi}^m}{\partial x} + \frac{\partial T_{yi}^m}{\partial y} + \frac{\partial T_{zi}^m}{\partial z} = -\frac{\partial T_{xi}^{mn}}{\partial x} - \frac{\partial T_{yi}^{mn}}{\partial y} - \frac{\partial T_{zi}^{mn}}{\partial z}, \quad i = x, y, z, \tag{5}$$

where the tensor containing the electric field components is given by

$$T_{ij}^m = u_j B_i - u_i B_j, \tag{6}$$

while the tensor expressing the QMHD correction term is determined by a combination of increments:

$$T_{ij}^{mn} = \Delta\left(T_{ij}^m\right) = B_i\Delta u_j + u_j\Delta B_i - B_j\Delta u_i - u_i\Delta B_j. \tag{7}$$

The total energy equation is

$$\frac{\partial E}{\partial t} + \frac{\partial F_x}{\partial x} + \frac{\partial F_y}{\partial y} + \frac{\partial F_z}{\partial z} + \frac{\partial Q_x}{\partial x} + \frac{\partial Q_y}{\partial y} + \frac{\partial Q_z}{\partial z} = \frac{\partial}{\partial x}\left(\Pi_{xx}u_x + \Pi_{xy}u_y + \Pi_{xz}u_z\right)$$
$$+ \frac{\partial}{\partial y}\left(\Pi_{yx}u_x + \Pi_{yy}u_y + \Pi_{yz}u_z\right) + \frac{\partial}{\partial z}\left(\Pi_{zx}u_x + \Pi_{zy}u_y + \Pi_{zz}u_z\right), \tag{8}$$

where

$$F_i = j_i\left(H + \frac{B^2}{2\rho}\right) - B_i\left(u_x B_x + u_y B_y + u_z B_z\right),$$

$$Q_i = -k\frac{\partial T}{\partial i} + \rho u_i\Delta\varepsilon + \rho u_i\left(p + B^2\right)\Delta\frac{1}{\rho}$$
$$+ u_i\left(B_x\Delta B_x + B_y\Delta B_y + B_z\Delta B_z\right) - B_i\left(B_x\Delta u_x + B_y\Delta u_y + B_z\Delta u_z\right).$$

Here, $i = x, y, z$ and $k$ is the thermal conductivity, which is determined in terms of $\mu$, $\gamma$, $R$, and the Prandtl number Pr:

$$k = \frac{\mu\gamma R}{(\gamma - 1)\mathrm{Pr}}.$$

Equations (2), (3), (5), and (8) make up the QMHD system. The parameters of the system are the ratio of specific heats $\gamma$, the dynamic viscosity $\mu$, the Prandtl number Pr, the mean molecular weight of the gas $\eta$, and the small regularizing parameter $\tau$. For rarefied gases, $\tau$ is naturally defined as

$$\tau = \alpha \frac{l}{c_f}, \tag{9}$$

where $l$ is the characteristic free path of gas molecules and $c_f = \max\left(c_f^x, c_f^y, c_f^z\right)$ is the maximum of the fast magnetosonic velocity. For example, the fast magnetosonic velocity in the $x$ direction is given by

$$c_f^x = \sqrt{\frac{1}{2}\left(c^2 + \frac{B^2}{\rho}\right) + \frac{1}{2}\sqrt{\left(c^2 + \frac{B^2}{\rho}\right)^2 - 4c^2\frac{B_x^2}{\rho}}},$$

where $c$ is the speed of sound:

$$c = \sqrt{\gamma p / \rho}.$$

The proportionality constant $\alpha$ in (9) is chosen in the range $0.1-0.4$. Definition (9) means that $\tau$ is the time over which a perturbation propagating at the maximum possible velocity travels a distance equal to the free path in the gas.

In the case of rarefied gases, $\tau$ is related to $\mu$ as

$$\mu = \tau p \, \text{Sc},$$

where Sc is the Schmidt number.

If the gas cannot be treated as rarefied, then, according to (9), $\tau \to 0$. If the physical processes weakly depend on the viscosity and thermal conductivity and the gas is not rarefied, then the QMHD equations pass into the standard MHD equation for an inviscid non-heat-conducting quasi-neutral gas. Written in conservative variables, these equations have the form (see [8])

$$\frac{\partial \mathbf{U}}{\partial t} + \frac{\partial \mathbf{F}}{\partial x} + \frac{\partial \mathbf{G}}{\partial y} + \frac{\partial \mathbf{H}}{\partial z} = 0,$$

where

$$\mathbf{U} = \begin{pmatrix} \rho \\ \rho u_x \\ \rho u_y \\ \rho u_z \\ B_x \\ B_y \\ B_z \\ E \end{pmatrix}, \quad \mathbf{F} = \begin{pmatrix} \rho u_x \\ \rho u_x^2 + p + \dfrac{B^2}{2} - B_x^2 \\ \rho u_x u_y - B_x B_y \\ \rho u_x u_z - B_x B_z \\ 0 \\ u_x B_y - u_y B_x \\ u_x B_z - u_z B_x \\ u_x\left(E + p + \dfrac{B^2}{2}\right) - B_x(\mathbf{u} \cdot \mathbf{B}) \end{pmatrix},$$

$$\mathbf{G} = \begin{pmatrix} \rho u_y \\ \rho u_x u_y - B_x B_y \\ \rho u_y^2 + p + \dfrac{B^2}{2} - B_y^2 \\ \rho u_y u_z - B_y B_z \\ u_y B_x - u_x B_y \\ 0 \\ u_y B_z - u_z B_y \\ u_y\left(E + p + \dfrac{B^2}{2}\right) - B_y(\mathbf{u} \cdot \mathbf{B}) \end{pmatrix}, \quad \mathbf{H} = \begin{pmatrix} \rho u_z \\ \rho u_x u_z - B_x B_z \\ \rho u_y u_z - B_y B_z \\ \rho u_z^2 + p + \dfrac{B^2}{2} - B_z^2 \\ u_z B_x - u_x B_z \\ u_z B_y - u_y B_z \\ 0 \\ u_z\left(E + p + \dfrac{B^2}{2}\right) - B_z(\mathbf{u} \cdot \mathbf{B}) \end{pmatrix}.$$
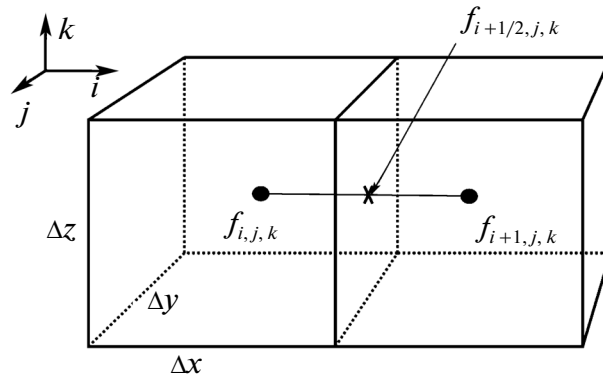
**Fig. 1.** Two adjacent grid cells with specified quantities.

For flows with low viscosity, for example, for ideal plasma flows, $\tau$ is a parameter of the numerical scheme. In this case, it plays an exclusively regularizing role and tends to zero as the cell size decreases.

Note that the QMHD equations do not contain terms proportional to the second time derivative, i.e., terms of the form $\sim\tau\partial^2/\partial t^2$. Formally, these terms can be written out when the original equations are averaged over time, but, in this paper, they are assumed to be small and are omitted (see [9]).

## 3. NUMERICAL ALGORITHM

The system of QMHD equations is solved numerically by applying an explicit difference scheme with derivatives approximated by central differences. We introduce a uniform grid that divides the computational domain into cells of size $\Delta x \times \Delta y \times \Delta z$, where $\Delta$ denotes the corresponding mesh size. The independent variables are placed at the cell centers and are denoted by integer indices $i$, $j$, and $k$, which correspond to the $x$, $y$, and $z$ directions. The half-integer indices denote quantities defined on cell interfaces. As an example, Fig. 1 shows two adjacent grid cells with quantities defined at their centers and on the interface between them.

When Eqs. (2), (3), (5), (8) are solved numerically, the time and space derivatives are replaced by difference expressions of the form

$$\frac{\partial f}{\partial t} \to \frac{\hat{f}_{i,j,k} - f_{i,j,k}}{\Delta t}, \quad \frac{\partial f}{\partial x} \to \frac{f_{i+1/2,j,k} - f_{i-1/2,j,k}}{\Delta x}, \quad (10)$$

where $\Delta t$ is the time step, $\hat{f}$ denotes the unknown quantities at the new time level $t + \Delta t$, and $f$ denotes the known quantities at the time level $t$. Rules (10) mean that the variations in the quantities within a cell are determined by the fluxes through its faces.

The time step is determined by the Courant condition

$$\Delta t = \sigma \min_{i,j,k}\left\{\frac{\Delta x}{|u_{xi,j,k}| + c^x_{fi,j,k}}, \frac{\Delta y}{|u_{yi,j,k}| + c^y_{fi,j,k}}, \frac{\Delta z}{|u_{zi,j,k}| + c^z_{fi,j,k}}\right\},$$

where $\sigma$ is the Courant number, which is determined experimentally and is no higher than 1.

Since the spatial derivatives in (2), (3), (5), and (8) involve quantities that are themselves determined by spatial derivatives, they are computed using differences between the centers of the adjacent cells:

$$\left.\frac{\partial f}{\partial x}\right|_{i+1/2,j,k} = \frac{f_{i+1,j,k} - f_{i,j,k}}{\Delta x}.$$

This means that the unknowns $\hat{f}$ placed at the cell center with index $(i, j, k)$ are computed using information from the adjacent cells with indices $(i \pm 1, j, k)$, $(i, j \pm 1, k)$, and $(i, j, k \pm 1)$. Thus, the stencil of the scheme consists of 27 points.
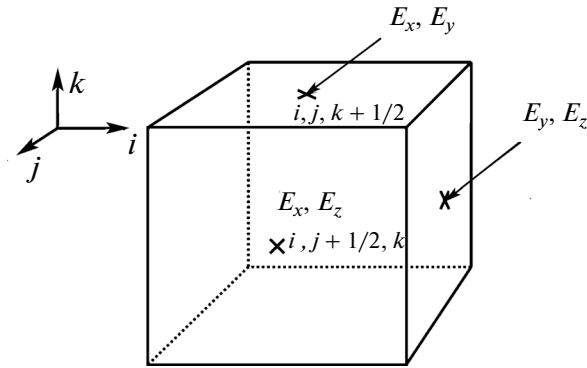
**Fig. 2.** Electric field components used in the magnetic field equations in the QMHD system.

The stability of the difference scheme is ensured by the regularizing parameters $\tau$, $\mu$, and $k$, which are proportional to the cell sizes:

$$\tau = \alpha \frac{h}{c_f}, \quad \mu = \tau p Sc, \quad k = \frac{\mu \gamma R}{(\gamma - 1) Pr},$$

where

$$h = \sqrt{\Delta x^2 + \Delta y^2 + \Delta z^2}.$$

## 4. DIVERGENCE-FREE MAGNETIC FIELD

In the simulation of magnetic flows, it is necessary to ensure that the computed magnetic field is free of divergence. For this purpose, we propose using the constrained transport method from [10]. The same method was used in [11] to construct a numerical scheme for computing MHD turbulence in an interstellar gas. The method is based on Faraday' law of induction

$$\partial \mathbf{B}/\partial t = -\mathrm{rot}\,\mathbf{E}, \tag{11}$$

where $\mathbf{E}$ is the vector of electric field strength. In the QMHD approach, Eqs. (5) are replaced by Eqs. (11), in which the electric field components are written taking into account the regularizing terms.

The electric field strength in matter moving at the velocity $\mathbf{u}$ is given by

$$\mathbf{E} = -[\mathbf{u}, \mathbf{B}].$$

Therefore, according to (6) and (7), the electric field components on corresponding ñell boundaries (see Fig. 2) are written in view of the QMHD correction terms as

$$E_{xi,j+1/2,k} = T_{yz}^{m} + T_{yz}^{mn}, \quad E_{xi,j,k+1/2} = -T_{zy}^{m} - T_{zy}^{mn}, E_{yi,j,k+1/2} = T_{zx}^{m} + T_{zx}^{mn},$$

$$E_{yi+1/2,j,k} = -T_{xz}^{m} - T_{xz}^{mn}, \quad E_{zi+1/2,j,k} = T_{xy}^{m} + T_{xy}^{mn}, \quad E_{zi,j+1/2,k} = -T_{yx}^{m} - T_{yx}^{mn}. \tag{12}$$

According to the constrained transport method, components (12) are transferred to the edge centers (see Fig. 3) using the formulas

$$E_{zi+1/2,j+1/2,k} = \frac{1}{4}\left(E_{zi+1/2,j,k} + E_{zi+1/2,j+1,k} + E_{zi,j+1/2,k} + E_{zi+1,j+1/2,k}\right)$$

$$+ \frac{\Delta y}{8}\left(\frac{\partial E_z}{\partial y}\bigg|_{i+1/2,j+1/4,k} - \frac{\partial E_z}{\partial y}\bigg|_{i+1/2,j+3/4,k}\right) + \frac{\Delta x}{8}\left(\frac{\partial E_z}{\partial x}\bigg|_{i+1/4,j+1/2,k} - \frac{\partial E_z}{\partial x}\bigg|_{i+3/4,j+1/2,k}\right),$$
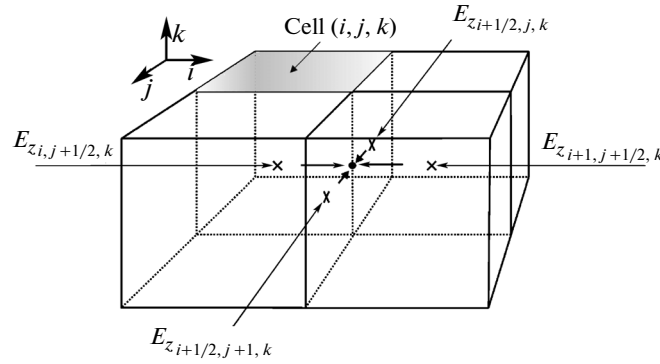
**Fig. 3.** Transfer of the electric field components from the centers of cell faces to the edge centers.
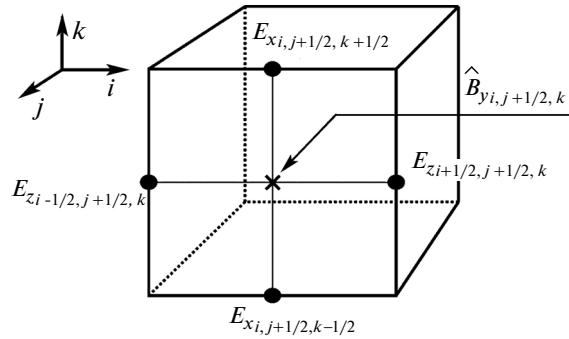


**Fig. 4.** Computation of the magnetic field components at the time level $t + \Delta t$ at the face centers according to Faraday's law of induction.

where the corresponding derivatives are calculated depending on the velocity sign on the face,

$$
\left. \frac{\partial E_z}{\partial y} \right|_{i+1/2, j+1/4, k} = \begin{cases} \left. \dfrac{\partial E_z}{\partial y} \right|_{i, j+1/4, k}, & u_{xi+1/2, j, k} > 0, \\[2ex] \left. \dfrac{\partial E_z}{\partial y} \right|_{i+1, j+1/4, k}, & u_{xi+1/2, j, k} < 0, \\[2ex] \dfrac{1}{2}\left( \left. \dfrac{\partial E_z}{\partial y} \right|_{i, j+1/4, k} + \left. \dfrac{\partial E_z}{\partial y} \right|_{i+1, j+1/4, k} \right), & \text{otherwise} \end{cases}
$$

with the use of difference expressions of the form

$$
\left. \frac{\partial E_z}{\partial y} \right|_{i, j+1/4, k} = 2\left( \frac{E_{zi, j+1/2, k} - E_{zi, j, k}}{\Delta y} \right).
$$

The resulting electric field components at the centers of cell edges are used in (11) to compute the magnetic field components at the centers of cell faces at the next time level $t + \Delta t$ (see Fig. 4). The difference approximation of (11) is given by

$$
\hat{B}_{xi+1/2, j, k} = B_{xi+1/2, j, k} - \frac{\Delta t}{\Delta y}\left( E_{zi+1/2, j+1/2, k} - E_{zi+1/2, j-1/2, k} \right) + \frac{\Delta t}{\Delta z}\left( E_{yi+1/2, j, k+1/2} - E_{yi+1/2, j, k-1/2} \right),
$$

$$
\hat{B}_{yi, j+1/2, k} = B_{yi, j+1/2, k} + \frac{\Delta t}{\Delta x}\left( E_{zi+1/2, j+1/2, k} - E_{zi-1/2, j+1/2, k} \right) - \frac{\Delta t}{\Delta z}\left( E_{xi, j+1/2, k+1/2} - E_{xi, j+1/2, k-1/2} \right),
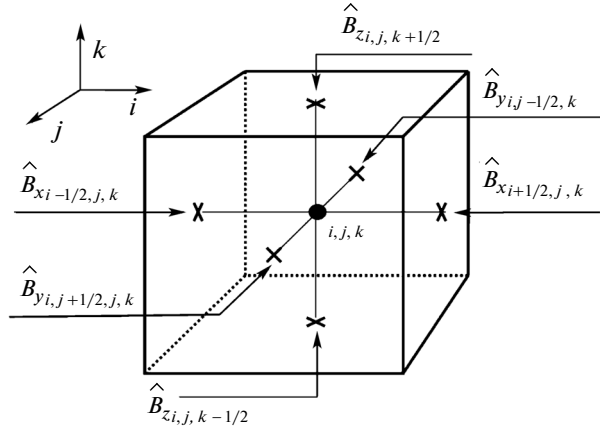$$

**Fig. 5.** Computation of the magnetic field components at the time level $t + \Delta t$ at the cell centers.

$$\hat{B}_{zi,j,k+1/2} = B_{yi,j,k+1/2} - \frac{\Delta t}{\Delta x}\left(E_{yi+1/2,j,k+1/2} - E_{yi-1/2,j,k+1/2}\right) + \frac{\Delta t}{\Delta y}\left(E_{xi,j+1/2,k+1/2} - E_{xi,j-1/2,k+1/2}\right).$$

The magnetic field components at the cell centers are calculated by simple averaging (Fig. 5):

$$\hat{B}_{xi,j,k} = \frac{1}{2}\left(\hat{B}_{xi+1/2,j,k} + \hat{B}_{xi-1/2,j,k}\right), \quad \hat{B}_{yi,j,k} = \frac{1}{2}\left(\hat{B}_{yi,j+1/2,k} + \hat{B}_{yi,j-1/2,k}\right), \quad \hat{B}_{zi,j,k} = \frac{1}{2}\left(\hat{B}_{zi,j,k+1/2} + \hat{B}_{xi,j,k-1/2}\right). \quad (13)$$

The magnetic field given by (13) is free of divergence. This can be seen by calculating the divergence at cell vertices using the formula

$$\text{div}\hat{\mathbf{B}}\Big|_{i+1/2,j+1/2,k+1/2} = \frac{1}{4\Delta x}\left(\hat{B}_{xi+1,j,k} - \hat{B}_{xi+1,j+1,k} - B_{xi,j,k} - B_{xi,j+1,k}\right)$$

$$+ \frac{1}{4\Delta x}\left(\hat{B}_{xi+1,j,k+1} + \hat{B}_{xi+1,j+1,k+1} - \hat{B}_{xi,j,k+1} - \hat{B}_{xi,j+1,k+1}\right)$$

$$+ \frac{1}{4\Delta y}\left(\hat{B}_{yi,j+1,k} + \hat{B}_{yi+1,j+1,k} - \hat{B}_{yi,j,k} - \hat{B}_{yi+1,j,k}\right) + \frac{1}{4\Delta y}\left(\hat{B}_{yi,j+1,k+1} + \hat{B}_{yi+1,j+1,k+1} - \hat{B}_{yi,j,k+1} - \hat{B}_{yi+1,j,k+1}\right)$$

$$+ \frac{1}{4\Delta z}\left(\hat{B}_{zi,j,k+1} + \hat{B}_{zi+1,j,k+1} - \hat{B}_{zi,j,k} - \hat{B}_{zi+1,j,k}\right) + \frac{1}{4\Delta z}\left(\hat{B}_{zi,j+1,k+1} + \hat{B}_{zi+1,j+1,k+1} - \hat{B}_{zi,j+1,k} - \hat{B}_{zi+1,j+1,k}\right).$$

## 5. NUMERICAL EXAMPLES

Below, we present the numerical results obtained by applying the method described to some popular MHD tests extended to three dimensions. The properties of the method as applied to one- and two-dimensional tests were analyzed numerically in [5, 6].

### 5.1. Blast in a Magnetic Field

The problem is to compute the structure of a perturbation caused by an excess pressure in a bounded domain as the perturbation travels through a medium with a magnetic field (blast wave problem) [12]. The computational domain was a cube with side $L = 1$, in which we introduced a uniform grid consisting of $120 \times 120 \times 120$ cells. Initially, the space was filled with an ideal gas with $\gamma = 1.4$, density $\rho = 1$, and pressure $p = 1$, except for the central spherical domain of radius $r = 0.05$, where the pressure was specified as $p = 1000$. In the $x$ direction, a homogeneous magnetic field $B_x = 10$ was applied (see Fig. 6). The computations were performed with $\alpha = 0.5$ and Courant number $\sigma = 0.1$.

The numerical results obtained at the time $t = 3 \times 10^{-2}$ are presented in Fig. 7. Specifically, the logarithm of density is shown in the form of a three-dimensional distribution and the two-dimensional cross
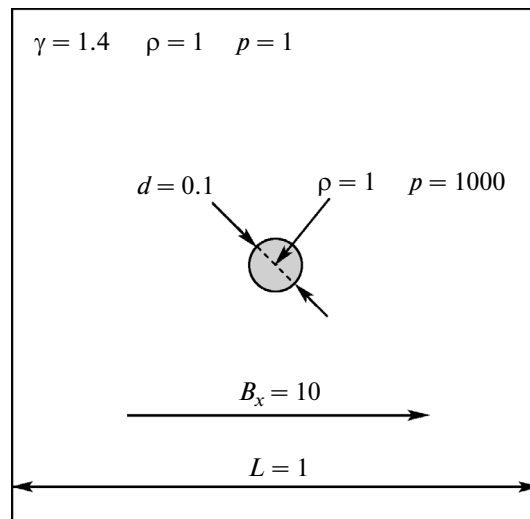
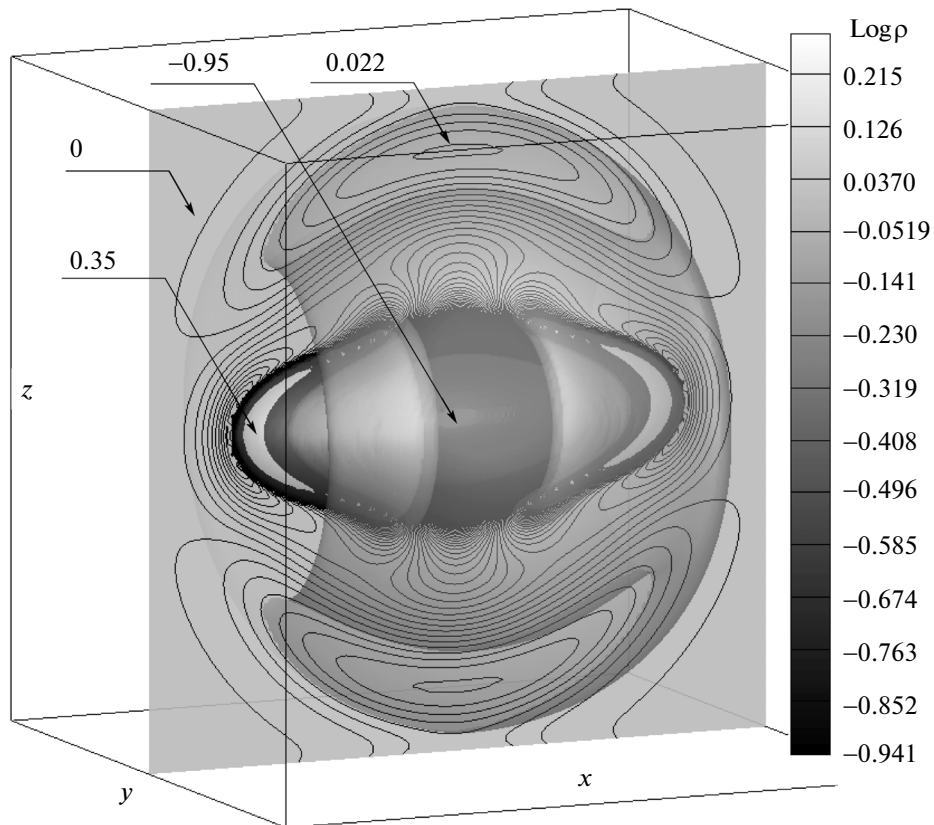**Fig. 6.** Blast in a magnetic field: initial conditions.



**Fig. 7.** Blast in a magnetic field. The logarithm of the density is shown as a three-dimensional distribution and the two-dimensional cross section in the plane $y = 0$ with level lines at the time $t = 3 \times 10^{-2}$. Additionally, the values in typical regions are indicated.

section along the plane $y = 0$ with level lines. Due to the magnetic pressure directed orthogonally to the field, the flow has a structure extended in the field direction. The maximum density $\log \rho \sim 0.35$ is reached in the areas of maximum medium resistance. Minimum values occur in the center: $\log \rho \sim -0.95$.
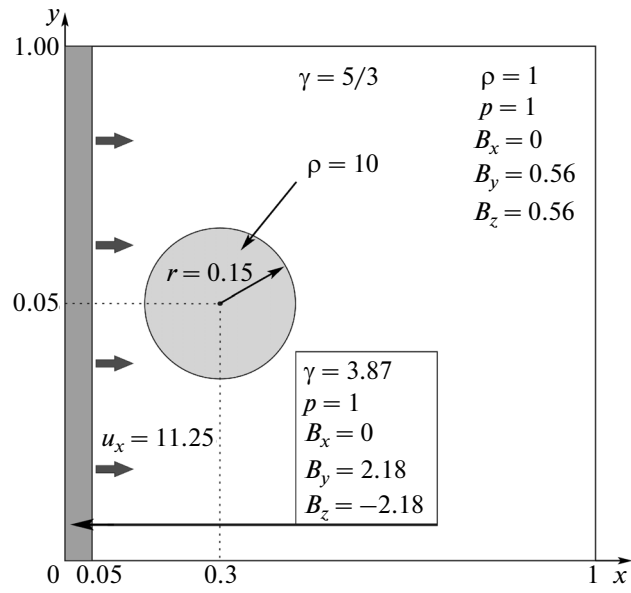
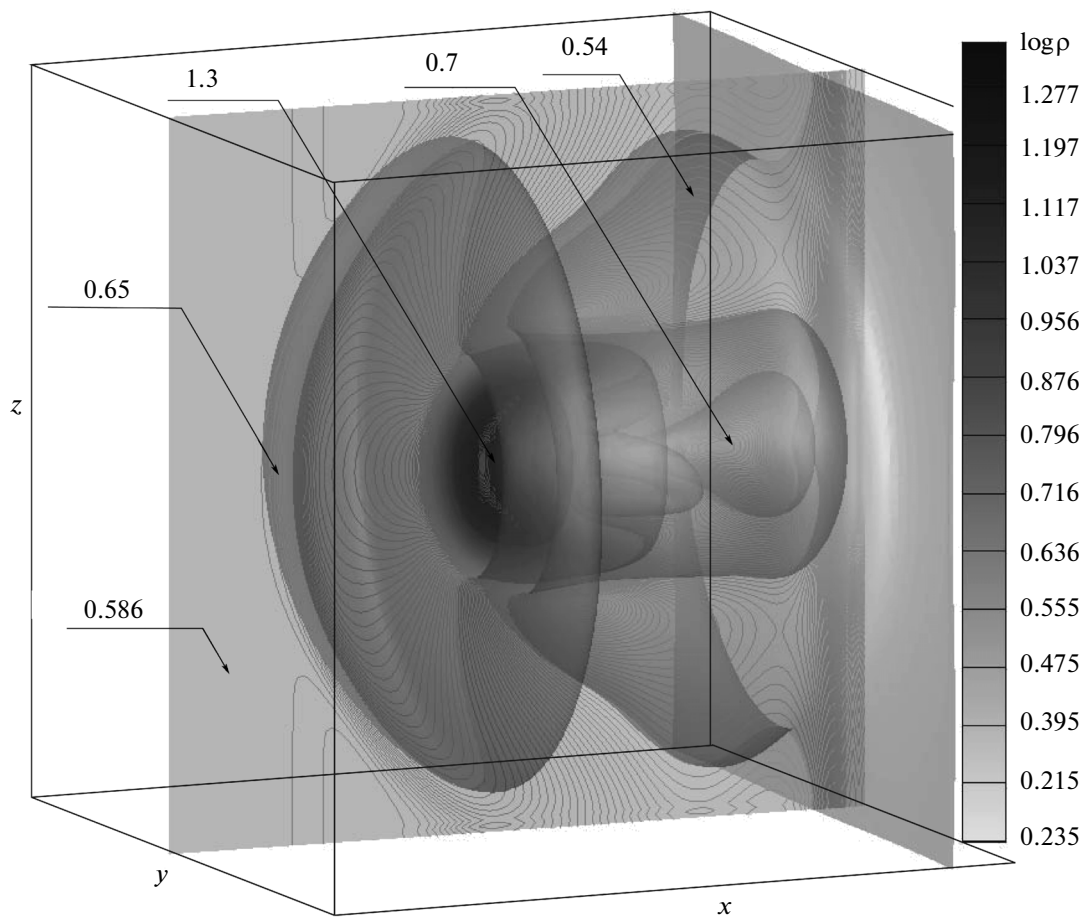**Fig. 8.** Interaction of a shock wave with a cloud: initial conditions.



**Fig. 9.** Interaction of a shock wave with a cloud. The logarithm of the density is shown as a three-dimensional distribution and the two-dimensional cross section in the plane $y = 0$ with level lines at the time $t = 6.09 \times 10^{-2}$. Additionally, the values in typical regions are indicated.
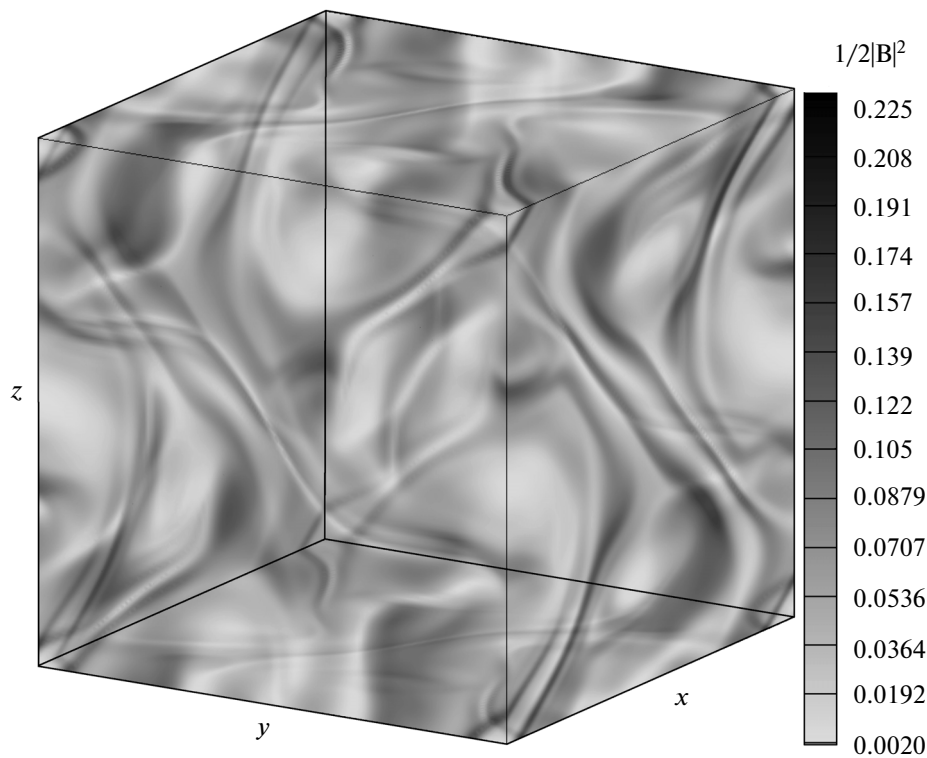
**Fig. 10.** Three-dimensional Orszag–Tang vortex: the magnetic field energy at the time $t = 0.5$.

### 5.2. Interaction of a Shock Wave with a Cloud

The problem is to compute the decay of a dense cloud interacting with a shock wave [13]. The computational domain was a cube with side $L = 1$, in which we introduced a uniform grid consisting of $120 \times 120 \times 120$ cells. The shock wave was initiated by a discontinuity between two states $\mathbf{U} = (\rho, u_x, u_y, u_z, B_x, B_y, B_z, p)$ separated by the plane $x = 0.05$:

$$U^L = (3.86859, 11.2536, 0, 0, 0, 2.1826182, -2.1826182, 167.345),$$
$$U^R = (1, 0, 0, 0, 0, 0.56418958, 0.56418958, 1).$$

A cloud of density $\rho = 10$ in a hydrostatic equilibrium with the surrounding medium was specified as a ball of radius $r = 0.15$ centered at the point $(x, y, z) = (0.3, 0.5, 0.5)$ (see Fig. 8). The computations were performed with $\alpha = 0.5$, $\sigma = 0.1$, and $\gamma = 5/3$.

The numerical results obtained at the time $t = 6.09 \times 10^{-2}$ are presented in Fig. 9. Specifically, the logarithm of density is shown in the form of a three-dimensional distribution and the two-dimensional cross section along the plane $y = 0$ with level lines. The resulting configuration reflects the hydrodynamic flow past an obstacle. Due to the resistance of the cloud to the flow, a hemispherical contact discontinuity arises ahead of the cloud. Behind the cloud, we see an anisotropic flow with a structure related to the direction of the magnetic field.

### 5.3. Three-Dimensional Orszag–Tang Vortex

This problem was first proposed in [14] in a two-dimensional formulation in order to study the evolution of supersonic turbulence and, later, became known as the Orszag–Tang vortex. Initially, smooth initial conditions are set, which rapidly give rise to a complex flow with the formation and interaction of shock waves. The problem is hard to solve for many numerical schemes, since the arising gradients, which are especially strong in the central part of the computational domain, can lead to oscillations and negative density values.
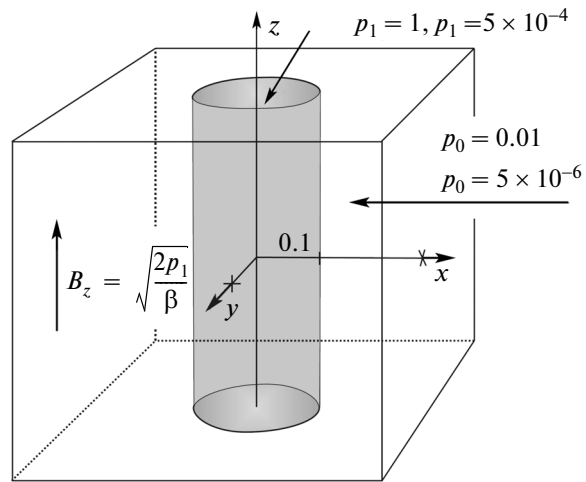
**Fig. 11.** Initial configuration of the plasma pinch in a magnetic trap.
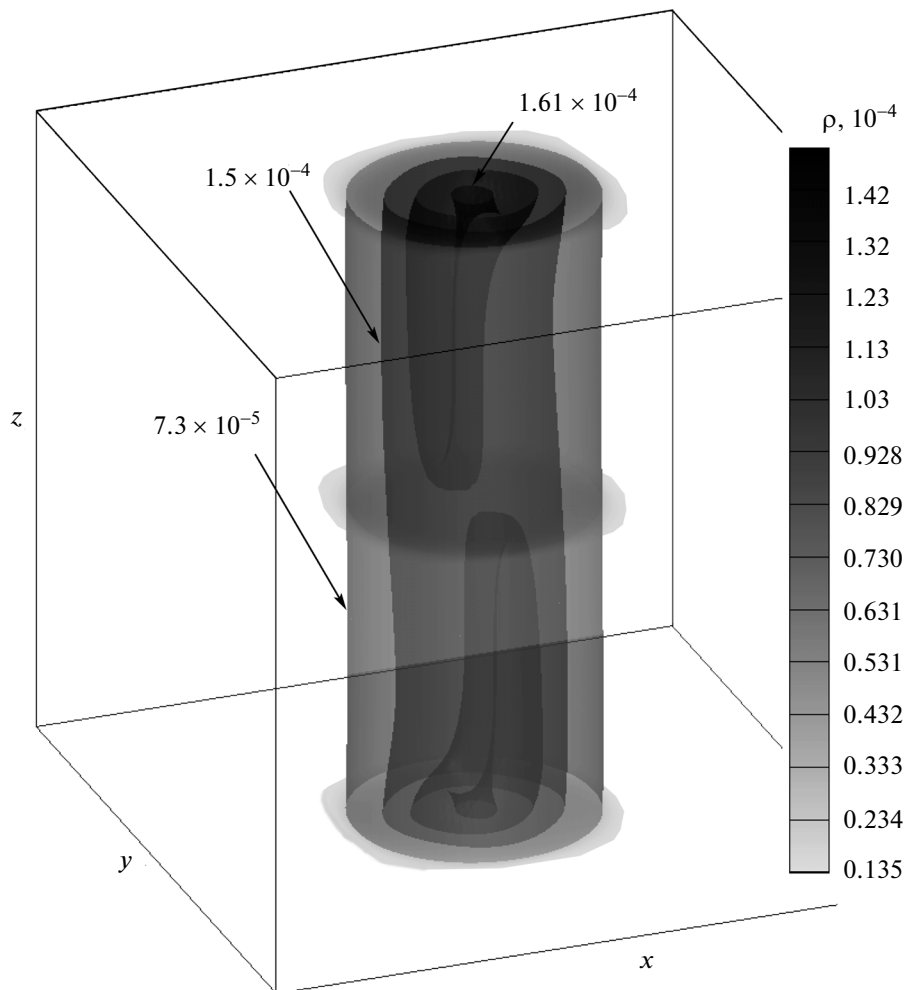


**Fig. 12.** Plasma pinch in a magnetic trap: density distribution with three characteristic levels $7.3 \times 10^{-5}$, $1.5 \times 10^{-4}$, and $1.61 \times 10^{-4}$ at some time.
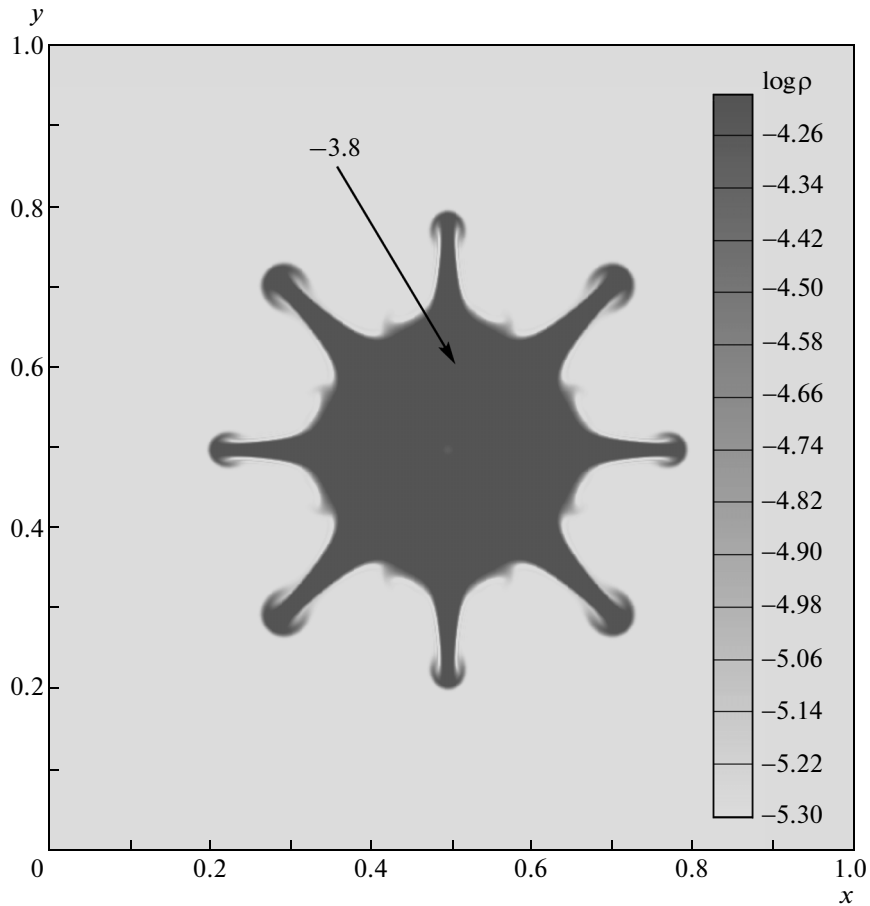
**Fig. 13.** Development of hydrodynamic instability in the pinch computed in the 2D formulation in the *xy* plane on a 400 × 400 grid. The density distribution at some time is shown on a logarithmic scale.

Below, this problem was considered in a three-dimensional formulation for the first time. The computational domain was a cube with side $L = 1$, in which we introduced a uniform grid consisting of $120 \times 120 \times 120$ cells. Periodic conditions were set on the boundary. The following initial conditions were proposed for the 3D case:

$$\rho = 25/(36\pi), \quad p = 5/(12\pi),$$
$$u_x = -\sin(2\pi z), \quad u_y = \sin(2\pi x), \quad u_z = \sin(2\pi y),$$
$$B_x = -B_0 \sin(2\pi z), \quad B_y = B_0 \sin(4\pi x), \quad B_z = B_0 \sin(4\pi y),$$

where $B_0 = 1/\sqrt{4\pi}$. The computations were performed with $\alpha = 0.5$, $\sigma = 0.1$, and $\gamma = 5/3$.

The numerical results obtained at the time $t = 0.5$ are presented in Fig. 10. Specifically, the energy of the magnetic field is shown by level lines in the range of 0.02 to 2.25. The method produces a correct flow structure with all discontinuities on an infinitely long time interval. As the computations continue, the flow gradually breaks up into small structures and its kinetic energy dissipates due to viscosity.

### 5.4. Confinement of a Plasma Pinch in a Magnetic Trap

The confinement of a hot plasma pinch in a trap with the help of a longitudinal magnetic field was simulated. Such a pinch is known as a $\theta$-pinch. A task of great interest from an engineering point of view, this problem concerns the creation of tokamak-type devices for thermonuclear fusion and has been addressed for several decades (see, e.g., [15, 16]). In experiments, the time of pinch confinement in a stable state is about several milliseconds, which is so short because of the development of hydrodynamic instability. We considered this process in a dimensionless formulation.

The computational domain was a cube with side $L = 1$ filled up with an ideal gas with $\gamma = 5/3$ (which corresponds to hydrogen), density $\rho_0 = 5 \times 10^{-6}$, and pressure $p_0 = 0.01$. A pinch was set in the center of the computational domain as a cylinder of radius $r = 0.1$ with inside characteristics $\rho_1 = 5 \times 10^{-4}$ and $p_1 = 1$. Initially, we specified the longitudinal magnetic field $B_z = \sqrt{2p_1/\beta}$, where $\beta = 5$. The initial configuration of the pinch is shown in Fig. 11. A uniform grid consisting of $120 \times 120 \times 120$ cells was introduced. The computations were performed with $\alpha = 0.5$ and $\sigma = 0.1$.

In the simulation, we obtained a cyclic process of plasma expansions and contractions under the influence of the magnetic pressure. Uniformly distributed at the initial time, the magnetic field was pushed out of the pinch region. Several cycles of direct and reverse energy flow between the magnetic field energy and the kinetic energy of the pinch matter were observed. The expansion of the plasma was suppressed by increasing the energy of the field.

To verify the stability of the code performance, we computed a pinch inclined initially to the $z$ axis at an angle of $\sim 10°$. As a result, the pinch aligned out along the magnetic field via cyclic oscillations. This process is demonstrated in Fig. 12, which shows the density distributions at some time with three characteristic levels: $7.3 \times 10^{-5}$, $1.5 \times 10^{-4}$, and $1.61 \times 10^{-4}$. It can be seen that the shape of the pinch is deformed in the oscillations.

In the three-dimensional case, we failed to resolve small-scale structures and simulate the development of instability because of the rather coarse grid used. Such instability was obtained when the pinch edge in the $xy$ plane was simulated on a $400 \times 400$ grid in the two-dimensional formulation. The instability developed transversely to the field direction and resembled the Rayleigh–Taylor instability. The structures generated in this process are demonstrated in Fig. 13, which displays the density distribution on a logarithmic scale at some time.

In the case of a weak magnetic field, no cyclic process or instability development was observed. The pinch broke up due to diffusion.

## 6. CONCLUSIONS

An algorithm for solving the QMHD equations describing unsteady compressible MHD flows with the ideal gas equation of state was presented. In contrast to earlier works, the QMHD equations were written is a self-consistent form within the framework of a unified approach to both conservation law equations in fluid dynamics and Faraday's laws for magnetic fields.

The scheme represented is fully three-dimensional, and all physical quantities are computed without splitting in space. The numerical algorithm was tested by computing several hard-to-solve three-dimensional MHD problems, on which the code exhibited an exceptionally stable performance. The chosen numerical parameter $\alpha = 0.5$ and the Courant number $\sigma = 0.1$ are universal for any problem.

The algorithm is easy to implement but rather cumbersome because of the additional monotonizing correction terms proportional to $\tau$. Due to the explicit scheme with central differences, the code was parallelized in a natural way by applying domain decomposition over the processors.

An advantage of the approach is that there is no need to use conventional monotonizing procedures, such as limiters, which are required in the case of the standard MHD equations. Such monotonizing procedures are not universal, so that the code has to be tuned in each particular case.

A shortcoming of the method is that it is first-order accurate, so finer grids have to be used to obtain solutions comparable in quality to those produced by high-order schemes. Note that the order of accuracy is determined by the solution behavior in smooth domains, while the most interesting are discontinuous solutions.

## REFERENCES

1. T. G. Elizarova, *Quasi-Gas Dynamic Equations* (Nauchnyi Mir, Moscow, 2007; Springer-Verlag, Berlin, 2009).

2. B. N. Chetverushkin, *Kinetic Schemes and Quasi-Gasdynamic System of Equations* (MAKS, Moscow, 2004; CIMNE, Barcelona, 2008).

3. Yu. V. Sheretov, *Continuum Dynamics under Spatiotemporal Averaging* (NITs Regulyarnaya i Khaoticheskaya Dinamika, Moscow, 2009).

4. T. G. Elizarova, I. S. Kalachinskaya, Yu. V. Sheretov, and I. A. Shirokov, "Numerical simulation of electrically conducting liquid flows in an external magnetic field," J. Commun. Technol. Electron. **50** (2), 227−233 (2005).

5. T. G. Elizarova and S. D. Ustyugov, Preprint No. 1, IPM RAN (Keldysh Inst. of Applied Mathematics, Russian Academy of Sciences, Moscow, 2011).

6. T. G. Elizarova and S. D. Ustyugov, Preprint No. 30, IPM RAN (Keldysh Inst. of Applied Mathematics, Russian Academy of Sciences, Moscow, 2011).

7. B. Ducomet and A. Zlotnik, "On a regularization of the magnetic gas dynamics system of equations," Kinetic Related Models **6** (3), 533−543 (2013).

8. A. G. Kulikovskii, N. V. Pogorelov, and A. Yu. Semenov, *Mathematical Aspects of Numerical Solution of Hyperbolic Systems* (Fizmatlit, Moscow, 2001; Chapman and Hall/CRC, London, 2001).

9. T. G. Elizarova, "Time averaging as an approximate technique for constructing quasi-gasdynamic and quasi-hydrodynamic equations," Comput. Math. Math. Phys. **51** (11), 1973−1982 (2011).

10. T. A. Gardiner and J. M. Stone, "An unsplit Godunov method for ideal MHD via constrained transport in three dimensions," J. Comput. Phys. **227**, 4123−4141 (2008).

11. S. D. Ustyugov, M. V. Popov, A. F. Kritsuk, and M. L. Norman, "Piecewise parabolic method on a local stencil for magnetized supersonic turbulence simulation," J. Comput. Phys. **228**, 7614−7633 (2009).

12. W. Dai and P. Woodward, "A simple finite difference scheme for multidimensional magnetohydrodynamical equations," J. Comput. Phys. **142**, 331−369 (1998).

13. G. Tóth, "The $\nabla \cdot \mathbf{B} = 0$ constraint in shock-capturing magnetohydrodynamics codes," J. Comput. Phys. **161**, 605−652 (2000).

14. S. A. Orszag and C.-M. Tang, "Small-scale structure of two-dimensional magnetohydrodynamic turbulence," J. Fluid Mech. **90**, 129−143 (1979).

15. A. A. Vedenov, E. P. Velikhov, and R. Z. Sagdeev, "Stability of plasma" Sov. Phys. Usp. **4**, 332−369 (1961).

16. V. E. Golant, A. P. Zhilinskii, and S. A. Sakharov, *Fundamentals of Plasma Physics* (Atomizdat, Moscow, 1977; Wiley, New York, 1980).

*Translated by I. Ruzanova*